Advanced high-strength steels for automotive engineering

Aleksandr Iurchenko[1*] and *Iurii* Simonov[1]

[1]Perm National Research Polytechnic University, Komsomolsky prospect, 29, 614000, Russia

Abstract. Diagrams of supercooled austenite decomposition are constructed for new steels of the Kh2G2C2MF alloying system. They provide the application of a science-based approach to the development and improvement of technological heat treatment processes with the use of furnaces with oxidising atmosphere. It is shown that the bainite transformation cannot exist separately from the martensite transformation even at slow cooling speeds. Regimes of heat treatment are selected, providing a possibility to receive the necessary structure for formation of a required complex of mechanical properties in a wide range. It is established that the most perspective heat treatment regime scheme from the point of view of time savings is continuous cooling from the heating temperature. It is revealed that the main structural components of steels after various heat treatment regimes are bainite and martensite, whose ratio determines the mechanical characteristics. Bainite is carbide-free, which favourably influences the complex of mechanical characteristics. The excessive ferrite and ferrite-carbide mixture formed in the structure at slow rates of continuous cooling in the upper temperature range do not affect the mechanical properties since their amount is insignificant. It is established that new economically alloyed steels with chromium, manganese, silicon, molybdenum, vanadium, and different carbon content belong to third-generation automotive steels, which gives prospects of using this material for manufacturing various automotive parts to improve the entire structure.

1 Introduction

In an era of rapid technological growth, the automotive industry is not standing still. In the wake of the increasing number of vehicles, it is necessary to maintain or even improve the quality of motor vehicle structures and components to improve human safety. Therefore, the automotive industry is actively introducing the 3rd Generation AHSS (Advanced High Strength Steels) [1-10, 21-22], which are used to manufacture high-strength body parts or longitudinal members, door parts, fasteners such as shear bolts, shafts [10-11].

The idea of third-generation high-strength steels dates back to the 90s of the last century when various automobile programmes were aimed at creating super-light, economical, safe for people and the environment [12]. Various automotive steel manufacturers in Japan, Germany, Sweden, and the United States took on the challenge of making the goal a reality

* Corresponding author: aleksmto@gmail.com

[12-13]. Since many global industrial companies are seeking to reduce the cost of steel production, new high-strength bainite steels [14], can compete with existing materials of different generations, which shows the relevance of the development of this direction.

High-strength bainite steels are systematically used abroad [1, 3-4, 15], having a low or near-average amount of carbon and containing silicon (1-2%), manganese, nickel, molybdenum and a small amount of chromium up to 1%. These steels are mainly used in the production of critical components such as axles, shafts, engine parts in the aerospace industry and heavy engineering. In the literature, there are also studies on steels with a high silicon content (up to 3%) but such information is rare. Furthermore, steels with a higher silicon content (up to 3%) are used in combination with a much higher manganese content (up to 12-14%) [10].

As shown in studies by the authors [14, 16], in economically alloyed steels such as Cr2SMF or Cr2H4MF with a carbon content of 0.2 to 0.3%, a carbide-free bainite structure is formed, providing a yield strength of 1100-1300 MPa, an ultimate strength of 1600-1800 MPa, and ductility is at the level of 13-25%. In this regard, the high structural strength of bainite-free bainite arouses interest in the study of bainite-free bainite alloys, which can be used in a number of critical structures, as well as in the automotive industry [7]. Furthermore, according to the authors of [8], high impact toughness can be obtained in massive steel parts with bainite-free bainite and limited carbon content in steel.

In Russia, Perm National Research Polytechnic University has developed new steels of the KH2G2C2MF alloying system with bainite structure [17-18]. Such alloying makes it possible to obtain an increased level of mechanical properties in steels after heat treatment in resistance furnaces rather than in bath furnaces. In this connection, the purpose of the work is to estimate the mechanical properties of the steels from the KH2G2C2MF alloying system after heat treatment in furnaces with an oxidising atmosphere with the possibility of their use as steels of the third generation for the automotive industry.

2 Materials and methods

The study materials were steels of the KH2G2C2MF alloying system, the chemical composition of which is presented in Table 1.

Table 1. Chemical composition of the study materials.

no	Steel grade	Chemical element content, % (wt.)									
		C	Cr	Mn	Si	Mo	V	S	P	Ni	Cu
1	17KH2G2C2MF	0.17	2.33	2.38	2.03	0.43	0.09	0.013	0.018	0.03	0.02
2	22KH2G2C2MF	0.22	2.36	2.40	2.06	0.39	0.09	0.014	0.022	0.33	0.18
3	29KH2G2C2MF	0.29	2.20	1.70	1.53	0.36	0.09	0.011	0.015	0.32	0.16
4	44KH2G2C2MF	0.44	2.31	2.19	2.18	0.36	0.09	0.012	0.015	0.31	0.16

Modeling of heat treatment regimes in order to draw diagrams of supercooled austenite decomposition was carried out on a Linseis L78 R.I.T.A. horizontal high-speed induction quenching dilatometer in high-purity helium (99.9999%) environment. Cylindrical samples with length of 10.0±0.05 mm and diameter of 3.0÷3.5 mm were used.

The initial structure was the hot forged state. Two types of thermal treatment regimes were carried out: thermal kinetic and isothermal. In the first case, heating of samples was carried out with the same heating rate (V_{HEAT}): V_{HEAT} = 1.5°C/s, austenitisation temperature (T_{AUST}) was 1000 °C, exposure time (τ_{EXP}) = 900 s at T_{AUST}, and the cooling rate (V_{COOL}) with T_{AUST} was in the range of 100 to 0.03 °C/s.

During isothermal treatment: V_{HEAT} = 1.5°C/s, T_{AUST} = 1000 °C, τ_{EXP} = 900 s, V_{COOL} = 1.5°C/s before and after the isothermal holding temperature (T_{ISO}) to room temperature (T_R). T_{ISO} and τ_{EXP} were different for each steel: T_{ISO} = 300-400 °C, τ_{EXP} = 6 h for 17KH2G2C2MF;

T_{ISO} = 275-375 °C, τ_{EXP} = 6 h for 22KH2G2C2MF; T_{ISO} = 250-400 °C, τ_{EXP} = 3 h for 29KH2G2C2MF; T_{ISO} = 200-325 °C, τ_{EXP} = 6 h for 44KH2G2C2MF.

Critical point position A_{C1} of the steels under study were determined by the moment of occurrence of the endothermic heat effect α→γ- The temperature of the end of austenite transformation, which increases the power required by the inductor of the dilatometer to maintain a given heating rate [19]. Temperature of end of austenite formation (A_{C_3}), the beginning and end of the bainite/martensite (B_b/M_b and B_e/M_e) transformations were determined by tear-off tangent to the linear section of the temperature dependence of the elongation of the sample.

A Buehler Micromet 6040 micro-hardness tangential diamond pyramid with a load of 100 grams was used to determine micro-hardness on dilatometric samples. ($HV_{0.1}$) and 20 gram ($HV_{0.02}$) considering GOST 9450-76.

The metallographic microstructure analysis was carried out with a light microscope (Olympus GX-51), a scanning microscope (Tescan Mira 3) and a transmission microscope (FEI Tecnai G2 30 S-TWIN) at magnifications from x100 to x60000. Preparation of microslips was carried out according to the standard technique. Etching surface of microslips for analysis on light and scanning microscopes was carried out by dipping method in reagents Nital and LePer. For transmission microscope microstructure analysis, thin blanks with a diameter of 3 mm and a thickness of 0.15 mm were prepared first, then these blanks were finally thinned by electrolytic thinning on the Tenupol-5 unit, followed by cleaning in the Fischione 1010 Ion Mill.

Experimental thermokinetic and isothermal regimes of thermal processing were carried out in chamber laboratory furnaces of resistance with oxidizing atmosphere "NAKAL". Heating to TAUST of steel billets 12×12×60 mm in size was carried out together with the furnace. Cooling during implementation of each treatment mode was always carried out in calm air. Two resistance furnaces were used to carry out isothermal treatment: in one of them heating to the austenitizing temperature was carried out, in the other one - holding in the area of bainite transformation. The TIZO temperature was assigned on the basis of the dilatometric results. Heat treatment time at PTA was regulated in order to ensure maximum flow of bainite transformation at PTA and to fit all heat treatment technology within one or two shifts in the plant's heat treatment shop. Each treatment mode was followed by low tempering: temperature T = 200 °C, τ_{EXP} = 2 h, cooling in still air.

For determination of impact toughness, we used pendulum-type tester KM-30, testing on which was carried out on specimens with the size 10x10x55 mm with V- and U-notch according to GOST 9454-78.

For determination of macro-hardness on halves of impact specimens used hardness TK-2M, measurements were conducted by Rockwell method (scale "C") in accordance with GOST 9013-59.

For determination of strength and ductility characteristics a tensile machine and INSTRON 5969 were used. Tests were conducted on type III specimens according to GOST 1497-84 with loading speed of 1 mm/min at room temperature.

X-ray diffraction analysis was carried out to determine residual austenite fraction (RASF) on halves of impact specimens on diffractometer DRON-3 using iron Kα-radiation at accelerating voltage 30kV and current strength 5 mA in the interval of angles 2θ from 53° to 59°. The volume fraction of austenite was calculated by the ratio of integral intensities of diffraction lines J(111) of austenite and J(110) of ferrite using the formula:

$$Ares, \% = \frac{100}{\left(\frac{J(110)\alpha}{J(111)\gamma}\right)*0.742+1},$$

here A_{res} is austenite residue fraction; $J_{(110)\alpha}$ is ferrite diffraction line intensity; $J_{(111)\gamma}$ is

intensity of the austenite diffraction line.

3 Results

The results of complex metallographic analysis have shown that the microstructure of the steels under study after different dilatometer heat treatment regimes mainly consists of bainite, which is carbide-free due to alloying the steels with the necessary amount of silicon, martensite and residual austenite (Fig. 1). In isolated cases (e.g., at a cooling rate of 0.05 ºC/s), ferrite is found in 17KH2G2C2MF steels, 22KH2G2C2MF and 29KH2G2C2MF steels, and a mixture of ferrite and carbide in steel 44KH2G2C2MF (Figure 1, a,b and Figure 2) occur, but in small amounts. In addition, areas of M/A are observed to show increased carbon content in these areas and consequently high austenite stability. The residual austenite is most often a film, which is enclosed between the alpha-phase plates (Figure 1, a). The lower bainite has a needle-like structure while the upper bainite, formed at the lowest cooling rates (the exception is steel 44KH2G2C2MF where all the bainite at the spent heat treatment regimes is lower), and also in the temperature range of isothermal curing 350-400 °C, has a needle-like structure.

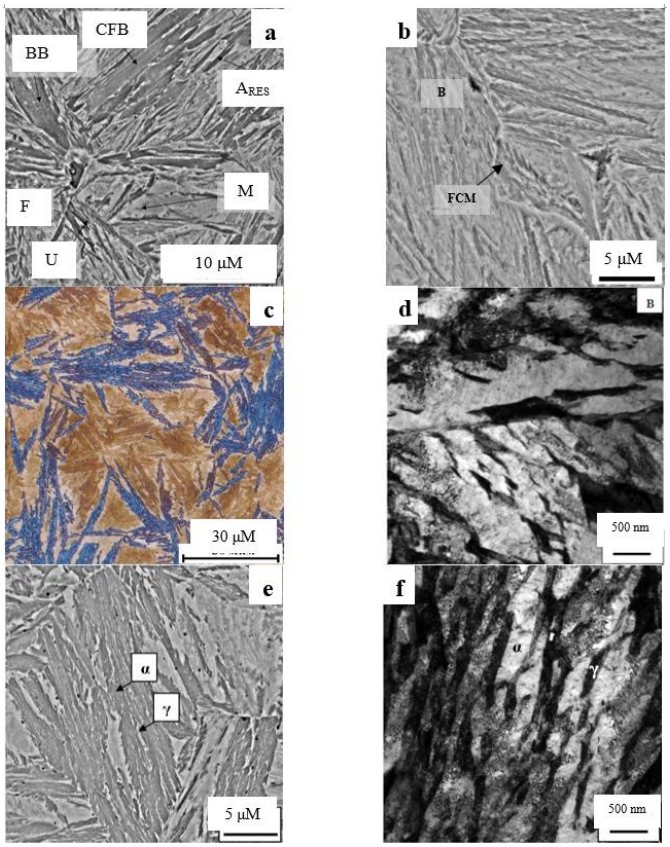

Fig. 1. Microstructure of 22KH2G2C2MF (a, c-d) and 44KH2G2C2MF (b, e-f) steels: a-b - V_{COOL} = 0.05 ºC/s; c-d – T_{ISO} = 375°C, τ_{exp} = 6 h; e-f – T_{ISO} = 325°C, τ_{exp} = 6 h; a-b, e – SEM; in – SM; d, f – TEM. CFB – carbide-free bainite, BB - bottom bainite, M_{REL} – martensite release, F - ferrite, UB - upper bainite, A_{RES} – residual austenite, M/A – martensite/austenite, B - bainite, FCM - ferrite-carbide mixture; a-b, e – etching with Nital reagent; etching with LePer reagent.

The decay diagrams of supercooled austenite show that the bainite transformation cannot exist separately from the martensitic transformation during continuous cooling, even at the slowest cooling rates (Figure 2). In steels with low carbon contents, the simultaneous martensitic-bainitic transformation proceeds in the range of cooling rates from 30 to 0.05°C/s, and in 44KH2G2C2MF steel it occurs only from 1.5°C/s and below. The temperature at which the bainite transformations begin decreases as the carbon content of the steels increases and the bainite zone shifts towards lower temperatures and cooling rates. An exception is 29KH2G2C2MF steel, which has a higher bainite transformation start temperature at low cooling rates than steels with lower carbon content (17KH2G2C2MF and 22KH2G2C2MF) in the thermokinetic diagram.

In 44KH2G2C2MF, the martensitic transformation proceeds up to room temperature throughout the range of cooling rates, and hence the martensitic transformation endpoint is below room temperature.

The overall microhardness level increases as the carbon content of the steel increases. As the cooling rate within each steel grade decreases, the micro-hardness level decreases. The micro-hardness level is consistent with the structure formed in each case.

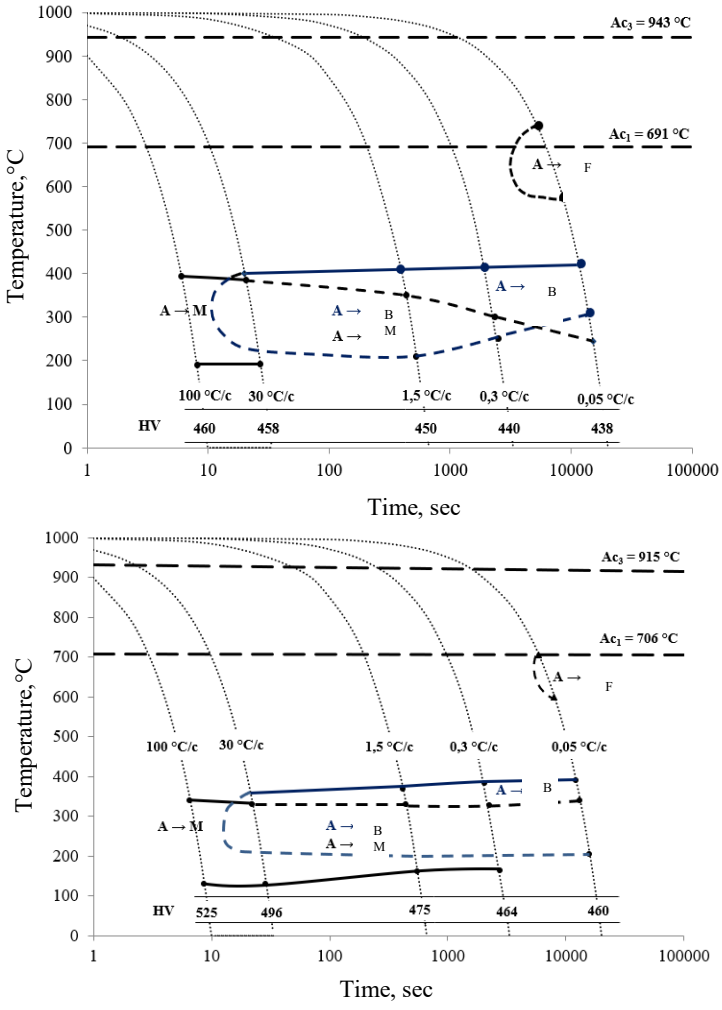

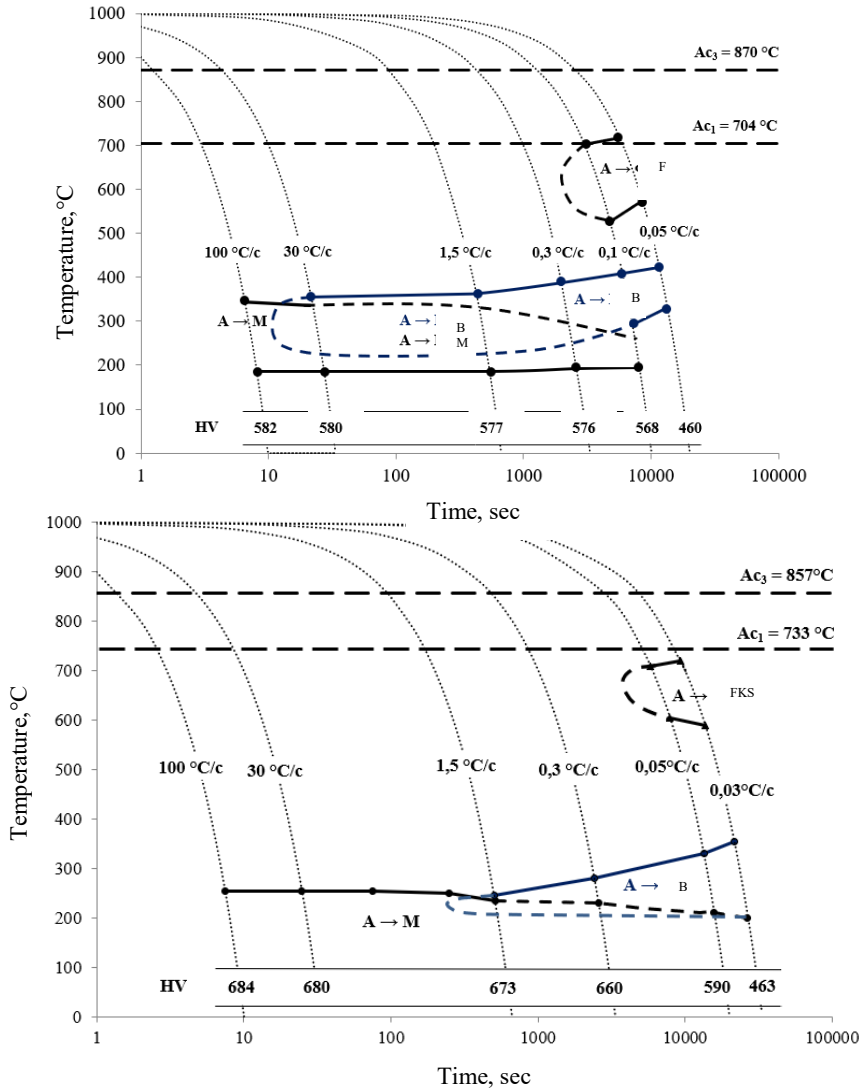

Fig. 2. Thermokinetic diagrams of supercooled austenite decomposition in 17KH2G2C2MF, 22KH2G2C2MF, 29KH2G2C2MF and 44KH2G2C2MF steels.

For the experimental heat treatment regimes, the hardening heating temperature of each steel was taken as the lowest possible temperature at which the mechanical properties start to change [20], and also taking into account the α-γ-transformation degree when determining A_{C3}. The aim was to reduce heating costs and heat treatment time without loss of mechanical properties, but with a bainite-martensitic structure.

As a result of heat treatment and mechanical tests, the KH2G2C2MF steels with a bainite-martensitic structure have a wide range of mechanical properties (Table 2). By varying the carbon content from 0.17 to 0.44%, the steels of the KH2G2C2MF alloying system can achieve high-strength (e.g., steels with 0.17-0.29% C) or ultra-high-strength (44KH2G2C2MF steel) conditions.

In steels containing 0.17-0.22% C, the mechanical properties are practically independent of the cooling rate within each steel grade. The proposed modes of isothermal treatment for

these steels do not lead to significant changes in the complex of mechanical properties. The exception is a decrease in relative elongation and impact toughness in steel 17KH2G2C2MF and, conversely, an increase in relative elongation and relative toughness in steel 22KH2G2C2MF.

The cooling rate of 29KH2G2C2MF steel significantly affects the strength characteristics, which decrease with decreasing cooling rate with virtually unchanged ductility and reliability. Among the isothermal heat treatment regimes, the intermediate isothermal holding temperature, namely 275°C, is worth mentioning. This temperature not only produces a high-strength condition but also increases the level of reliability compared to other temperatures. The same situation is observed in 44KH2G2C2MF steel, the soaking at 275°C results in the formation of optimum properties among the conducted isothermal heat treatment regimes. However, the mechanical properties after continuous cooling of medium-carbon steel cannot be overlooked. At the highest tensile strength limit, the relative elongation and contraction of the steel in this condition is reduced by only a few percent, and the impact toughness is not different from that of isothermal heat treatment regimes.

The graphs in Figure 3 show that, in terms of the combination of impact toughness KCV and yield strength, impact toughness KCV and $\sigma_{0.2}/\sigma_a$ Steels with a low carbon content have an increased range of properties (at KCV=0.35-0.55 MJ/m^2 yield strength is 1000-1400 MPa, $\sigma_{0.2}/\sigma_a$ is 0.6-0.8) compared to 44KH2G2C2MF steel (Figure 3). However, in terms of combination of ultimate strength and relative elongation, most of the steel values after all heat treatment regimes are concentrated in the region corresponding to the mechanical properties of third-generation automotive steels (Figure 4). In addition, the property values of steel with 0.44 % carbon not only fall within the required range but also exceed the range with a promising margin immediately after continuous cooling from the austenitizing temperature. It should be noted that it is in steel 44KH2G2C2MF that the greatest amount of residual austenite is observed after heat treatment of the steels, being in the range of 19 to 27 % (Table 2).

Table 2. Mechanical properties of steels of the KH2G2C2MF alloying system after continuous cooling and isothermal treatment.

Processing mode	$\sigma_{0.2}$	σ_a	δ	Ψ	KCV	KCU	HRC	$\sigma_{0.2}/\sigma_a$	A_{RES}, %
	MPa		%		MJ/m^2				
17KH2G2C2MF									
T_{AUST} = 900°C, air	1220	1520	12.0	48.5	0.51	0.95	42	0.80	<5
T_{AUST} = 900°C, s	1140	1460	12.5	45.5	0.42	1.05	39	0.79	<5
T_{AUST} = 900°C, T_{ISO} = 350°C (3 h)	1210	1570	13.0	38.0	0.35	0.68	43	0.77	<5
22KH2G2C2MF									
T_{AUST} = 880°C, air	1310	1670	11.5	35.0	0.44	0.70	46	0.78	8
T_{AUST} = 880°C, s	1280	1580	11.5	38.0	0.43	0.84	43	0.81	12
T_{AUST} = 880°C, T_{ISO} = 300°C (6 h)	1180	1610	16.5	43.0	0.38	0.70	44	0.73	13
29KH2G2C2MF									
T_{AUST} = 880°C, air	1420	1790	15.0	44.0	0.38	0.82	45	0.79	9
T_{AUST} = 880°C, s	1090	1480	14.5	41.5	0.41	0.93	40	0.74	<5
T_{AUST} = 880°C, T_{ISO} = 325°C (6 h)	1000	1530	15.5	43.0	0.38	-	46	0.66	15
T_{AUST} = 880°C, T_{ISO} = 300°C (6 h)	1090	1520	15.5	48.0	0.38	-	46	0.72	7
T_{AUST} = 880°C, T_{ISO} = 275°C (6 h)	1310	1650	13.5	50.5	0.53	0.94	45	0.79	8
T_{AUST} = 880°C, T_{ISO} = 250°C (6 h)	1070	1610	11.5	43.0	0.42	-	47	0.66	<5

44KH2G2C2MF									
T_{AUST} = 860°C, air	1480	2200	9.0	14.0	0.20	-	55	0.67	22
T_{AUST} = 860°C, T_{ISO} = 325°C (6 h)	940	1810	13.0	12.0	0.17	-	48	0.52	27
T_{AUST} = 860°C, T_{ISO} = 300°C (6 h)	980	1750	16.0	20.0	0.22	-	49	0.56	26
T_{AUST} = 860°C, T_{ISO} = 275°C (6 h)	1100	1870	14.0	21.0	0.21	-	50	0.60	19
T_{AUST} = 860°C, T_{ISO} = 250°C (6 h)	1000	1970	11.0	13.0	0.18	-	51	0.50	20
Note. Each treatment was followed by tempering at 200 °C with an exposure time of 120 min and air cooling									

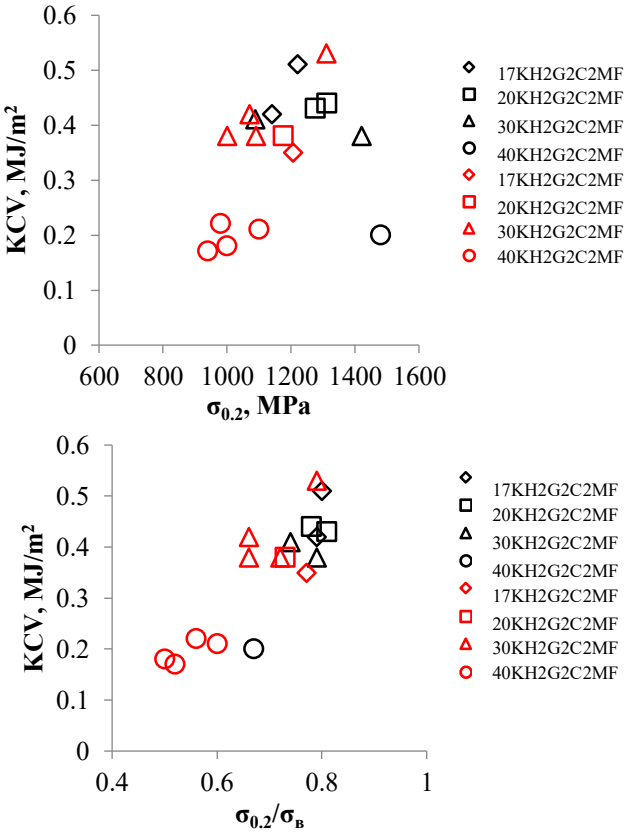

Fig. 3. Impact toughness versus yield strength (a) and yield strength versus tensile strength ratio (b). Black figures - continuous cooling; orange figures - isothermal treatment.

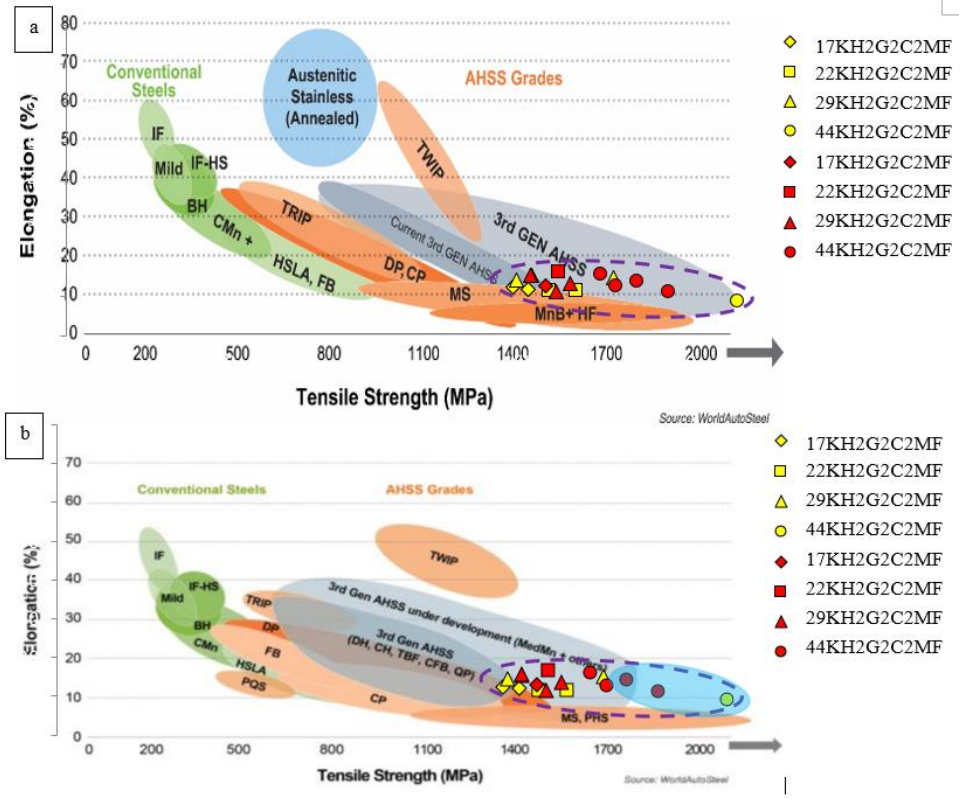

Fig. 4. Steel Strength Ductility Diagram (2017) [23] (a) and The Global Formability Diagram (2021) (b) comparing strength and elongation of current and emerging steel grades [24] with the plotted experimental results obtained in this paper. Yellow figures are continuous cooling; red figures are isothermal treatment.

4 Discussions

According to metallographic analysis by scanning and transmission microscopy, the presence of bainite without carbide was established in the structure, which was found to be beneficial for the formation of a set of mechanical characteristics in the new steels. Therefore, obtaining such a structural component in such grades will have a positive effect when they are used in vehicle construction.

Due to the fact that KH2G2C2MF steels are alloyed with manganese, silicon and molybdenum, the stability of austenite is increased and, as a consequence, the formation of excess phases in the high-temperature region is unlikely. Therefore, excess ferrite is formed only at the lowest cooling rates. In 44KH2G2C2MF steel, austenite transformation is carried out in a ferrite-carbide mixture due to a sufficiently high carbon content.

It is known that the silicon content affects the onset temperature of the bainite transformation. The bainite transformation initiation temperatures differ in the steels studied, especially at the slowest continuous cooling rates. The increased silicon content with the greatest amount of carbon in steel 44KH2G2C2MF resulted in a lower bainite transformation initiation temperature and a narrowing of the bainite transformation temperature interval. In 29KH2G2C2MF steel, the amount of silicon is the lowest among all steels, however, with higher carbon content compared to 17KH2G2C2MF and 22KH2G2C2MF steel, the bainite transformation start temperature is in the same range as in 17KH2G2C2MF and

22KH2G2C2MF steel.

The silicon content not only influenced the decrease in the initiation temperature of the bainite transformation but also shifted the bainite transformation in general to the martensitic interval. Thus, it is expected that a bainite-martensitic structure will always develop in these steels in any heat treatment condition. This is an advantage of such steels because it allows the mechanical characteristics to be adjusted by obtaining the desired ratio of martensite to bainite, especially during isothermal treatment.

One of the important characteristics of high-strength steels is the stability of retained austenite. The closer to unity the ratio of yield strength to tensile strength, the greater the stability of residual austenite under mechanical action. Basically, the ratio $\sigma_{0.2}/\sigma_a$ is consistently in the range of 0.6 to 0.8 at different heat treatment finishes. However, in the steel 44KH2G2C2MF the ratio $\sigma_{0.2}/\sigma_a$ decreases to 0.5-0.6. This steel acquires an increased level of ductility as a result of the trip effect, which manifests itself in the tensile process. In this case there is a local conversion of residual austenite, the amount of which is greater in this steel (Table 2), into martensite.

Among the modes of final heat treatment, two groups should be distinguished: continuous cooling from austenitizing temperatures and isothermal treatment in the bainite transformation region. The main and main advantage of the first group is the ease of heat treatment of steels. It is especially important, when these heat treatment regimes are carried out in furnaces with oxidizing atmosphere and the use of air for cooling. This, in turn, avoids the cost of quenching tanks and the use of salt bath furnaces for isothermal treatment regimes, which are harmful.

A key part of this work is to determine the possibility of using new economically alloyed steels with chromium, manganese, silicon, molybdenum, and vanadium as third-generation automotive steels. These steels are not only ranked third-generation steels in terms of strength and ductility, as shown in the 2017 and 2021 strength and ductility diagrams (Figure 4), but will also be firmly anchored in this category for years to come, with their safety margin and potential for further improvement without a marked reduction in ductility and toughness characteristics. Additionally, once the experimental points have been plotted on the current automotive steel classification diagram, it can be seen that some of the points seem to form a new area highlighted in blue in the diagram (Fig. 4, b). Thus, this area could in the future have the status of a separate class of automotive steels, especially if the level of ductility is slightly increased, e.g., up to 20% while maintaining strength by selecting an appropriate heat treatment regime.

5 Conclusions

1. Diagrams of supercooled austenite decomposition for new steels of KH2G2C2MF alloying system are constructed, allowing to apply science-based approach to development and improvement of heat treatment technological processes using furnaces with oxidizing atmosphere. It is shown that the bainite transformation cannot exist separately from the martensitic transformation even at slow speeds of cooling.
2. The heat treatment regimes allowing getting necessary structure for forming of required complex of mechanical properties in wide range are selected and approved. The most perspective heat treatment regime scheme from the viewpoint of time saving is continuous cooling in calm air from the heating temperature.
3. The basic structural components of steels after various heat treatment regimes are bainite and martensite, the ratio of which determines the mechanical characteristics.
4. The new steels of alloying system KH2G2C2MF belong to the automotive high-strength steels of third generation, which gives prospects of using this material for making various parts of automobiles in order to improve the whole structure.

Acknowledgement

The research was carried out with the financial support of the Government of Perm Krai within the framework of scientific project No. C26/513.

References

1. J-H. Kima, D. Kima, H.N. Hanb et al, Materials Science & Engineering **A559**, 222-231 (2013)
2. M.V. Maisuradze, M.A. Ryzhkov, Metallurgist **62**, 337-347 (2018)
3. Qin, S., Liu Y., Hao, Q. et al, Metallurgical and materials transactions **47A**, 4853-4861 (2016)
4. L. Heping, S. Feng'er, S. Hu'er, et al, Journal of Wuhan University of Technology-Mater. Sci. Ed. **31.5**, 1099-1104 (2016)
5. N. Baluch, Z.M. Udin, C.S. Abdullah, Engineering, technology & applied science research **4.4**, 686-689 (2014)
6. H.R. Ghazvinloo, A. Honarbakhsh-Raouf, Materials Science **52.4**, 572-579 (2017)
7. F.G. Caballero, S. Allain, J. Cornide et al Materials and design **49**, 667-680 (2013)
8. T. Nanda, V. Singh, G. Singh, et al, Archives of civil and mechanical engineering **21.7**, 6-24 (2021)
9. K. Radwański, Archives of civil and mechanical engineering **16**, 282-293 (2016)
10. W. Bleck, F. Brühl, Y. Ma, C. Sasse, Berg huettenmaenn monatsh **164.11**, 466-474 (2019)
11. V.E. Telegin, S.G. Sinitsky, O.V. Andreev, Steel **9**, 53-56 (2018)
12. S.M. Kudryavtsev, G.V. Pachurin, D.V. Solovyov, *Fundamentals of design, production and materials of modern car body: monograph* (2010)
13. Y.F. Ivanov, V.E. Gromov, E.N. Nikitina, Bainite structural steel: structure and strengthening mechanisms **179** (2015)
14. F.G. Caballero, M.J. Santofimia, C. García-Mateo, Materials and design **30.6**, 2077-2083 (2009)
15. M.V. Maisuradze, M.A. Ryzhkov, O.A. Surnaeva, Steel **6**, 62-66 (2016)
16. F.G. Caballero, H.K.D.H. Bhadeshia, K.J.A. Mawella, Materials science and technology **17**, 517-522 (2001)
17. A.N. Yurchenko, Yu.N. Simonov, D.O. Panov, A.I. Zhitenev, Metal science and heat treatment **61**, 617–621 (2020)
18. A.N. Yurchenko, Yu.N. Simonov, O.V. Efimova, Metal science and heat treatment **61**, 622–627 (2020)
19. D.O. Panov, Y.N. Simonov, L.V. Spivak, A.I. Smirnov, The physics of metals and metallography **116**, 802–809 (2015)
20. A.N. Yurchenko, M.A. Marieva, R.D. Grebenkin, Y.N. Simonov, Bulletin of Perm National Research Polytechnic University "Engineering, Materials Science" **21.3**, 85-92 (2019)
21. R.K. Verma, D. Bhattacharjee, Trans Indian Inst Met **74.5**, 1173–1178 (2021)
22. D. Fro´meta, A. Lara, L. Grife´ et al, Metallurgical and materials transactions **52A**, 840-856 (2021)

23. A new global formability diagram, URL: https://ahssinsights.org/blog/a-new-global-formability-diagram/
24. Advanced High-Strength Steel (AHSS) definitions, URL: https://www.worldautosteel.org/steel-basics/automotive-advanced-high-strength-steel-ahss-definitions/